TU Delft

Delft University of Technology

A Macroscopic Flow Model for Mixed Bicycle–Car Traffic

Wierbos, Marie-Jette; Knoop, Victor; Hanseler, Flurin; Hoogendoorn, Serge

DOI
10.1080/23249935.2019.1708512

Publication date
2020

Document Version
Final published version

Published in
Transportmetrica A: Transport Science

Citation (APA)
Wierbos, M.-J., Knoop, V., Hanseler, F., & Hoogendoorn, S. (2020). A Macroscopic Flow Model for Mixed Bicycle–Car Traffic. *Transportmetrica A: Transport Science*, *17*(3), 340-355. https://doi.org/10.1080/23249935.2019.1708512

Important note
To cite this publication, please use the final published version (if applicable).
Please check the document version above.

Copyright
Other than for strictly personal use, it is not permitted to download, forward or distribute the text or part of it, without the consent of the author(s) and/or copyright holder(s), unless the work is under an open content license such as Creative Commons.

Takedown policy
Please contact us and provide details if you believe this document breaches copyrights.
We will remove access to the work immediately and investigate your claim.

This work is downloaded from Delft University of Technology.
For technical reasons the number of authors shown on this cover page is limited to a maximum of 10.

Taylor & Francis
Taylor & Francis Group

Transportmetrica A: Transport Science

ISSN: (Print) (Online) Journal homepage: https://www.tandfonline.com/loi/ttra21

A macroscopic flow model for mixed bicycle–car traffic

M. J. Wierbos , V. L. Knoop , F. S. Hänseler & S. P. Hoogendoorn

To cite this article: M. J. Wierbos , V. L. Knoop , F. S. Hänseler & S. P. Hoogendoorn (2021) A macroscopic flow model for mixed bicycle–car traffic, Transportmetrica A: Transport Science, 17:3, 340-355, DOI: 10.1080/23249935.2019.1708512

To link to this article: https://doi.org/10.1080/23249935.2019.1708512

© 2020 The Author(s). Published by Informa UK Limited, trading as Taylor & Francis Group

Published online: 04 Jan 2020.

Submit your article to this journal

Article views: 747

View related articles

View Crossmark data

Citing articles: 1 View citing articles

Full Terms & Conditions of access and use can be found at
https://www.tandfonline.com/action/journalInformation?journalCode=ttra21

TRANSPORTMETRICA A: TRANSPORT SCIENCE
2021, VOL. 17, NO. 3, 340–355
https://doi.org/10.1080/23249935.2019.1708512

Taylor & Francis
Taylor & Francis Group

OPEN ACCESS Check for updates

A macroscopic flow model for mixed bicycle–car traffic

M. J. Wierbos, V. L. Knoop, F. S. Hänseler and S. P. Hoogendoorn

Department of Transport and Planning, Delft University of Technology, Delft, The Netherlands

ABSTRACT

Bicycles are gaining popularity as a mode of transport resulting in a mixed bicycle–car traffic situation on urban roads. Cyclists, however, are hardly included in traffic flow models which complicates the design of safe and congestion-free traffic situations. This work introduces class-specific speed functions based on two variables, being space headway for both cars and cyclists. This enables the macroscopic modelling of mixed bicycle–car traffic. The multi-class macroscopic flow model is successfully tested for different traffic situations that occur on urban roads where cyclists and cars share the same infrastructure, e.g. cyclists overtaking a queue of cars and cars overtaking cyclists with reduced speed. The mixed bicycle–car flow model allows travel time estimation of both classes, which in turn can be used to evaluate the overall performance of a mixed traffic road.

ARTICLE HISTORY
Received 31 December 2018
Accepted 29 November 2019

KEYWORDS
Macroscopic flow model; mixed traffic; bicycle; class-specific speed function

1. Introduction

Traffic participants in urban environments often share the available infrastructure. In places with high cyclist volumes, the roads are used simultaneously by cars and cyclists. This creates a mixed traffic situation in which both classes can be the fastest moving one depending on the traffic state. In low demand situations, cars have the opportunity to overtake cyclists, while in congested situations, the cyclists can manoeuvre alongside a queue of cars and thus be the fastest moving class. An essential property of mixed traffic flow is this ability of cyclists to continue moving in congested traffic. Describing this feature is important for estimating the expected travel time loss, which is a common metric for road network performance. The travel time loss may differ for the multiple user types since the experienced delay depends on the traffic state and the specific class characteristics.

Macroscopic flow models are commonly used for travel time estimation. However, these models generally handle mixed traffic situations by selecting cars as the reference class and expressing the other classes in passenger car equivalents (pce) based on their impact to the traffic flow. The pce-concept was first introduced in the U.S. Highway Capacity Manual by (National Research Council 1965) and has been used in many studies since then resulting in various methods to convert a mixed traffic stream into a uniform one, as summarised by Shalini and Kumar (2014). A consequence of using the pce-concept is that the

CONTACT M. J. Wierbos m.j.wierbos@tudelft.nl Department of Transport and Planning, Delft University of Technology, Stevinweg 1, Delft, The Netherlands

© 2020 The Author(s). Published by Informa UK Limited, trading as Taylor & Francis Group
This is an Open Access article distributed under the terms of the Creative Commons Attribution-NonCommercial-NoDerivatives License (http://creativecommons.org/licenses/by-nc-nd/4.0/), which permits non-commercial re-use, distribution, and reproduction in any medium, provided the original work is properly cited, and is not altered, transformed, or built upon in any way.

speeds for both classes depend on one (pce-based) density, and cannot depend on the vehicle-bicycle composition leading to that density. Therefore, it does not fully represent the movements observed in mixed bicycle–car traffic. Our purpose here is to overcome this limiting model property by introducing an alternative approach that enables switching of the fastest moving class in congestion.

This work presents a multi-class macroscopic traffic flow model which uses class-specific speed functions that depend on the density of all classes as independent variables. The distinction into classes is based on the mode of transportation only, so heterogeneity in e.g. driver type is not considered. A Lagrangian approach is used, following groups of traffic participants over time. Both group size and simulation time are discretised in the numerical implementation, while position is a continuum. The class-specific speed functions are two-dimensional and take into account the space headway of both cars and cyclists. The successful working of the model is illustrated for different traffic situations that typically occur on urban roads. The proposed model allows for travel time estimation for multiple traffic modes by describing their joint traffic dynamics, which in turn can be used to evaluate the overall performance of a mixed traffic road.

The paper continues with a background on macroscopic traffic flow modelling in Section 2, followed by an explanation of the modelling principles in Section 3, the numerical implementation of the model in Section 4 and the presentation of the class-specific speed functions in Section 5. Afterwards, Section 6 illustrates the successful working of the model and Section 7 presents the discussion and conclusion.

2. Background on macroscopic modelling

This paper aims to describe mixed traffic flow in an urban setting where cars and cyclists share the infrastructure, using a macroscopic flow model. Macroscopic models describe the evolution of traffic movements over time and space at an aggregated scale using the quantities: density, average speed and flow. This differs from microscopic flow models, which describe the movements of individual traffic participants. The distinction between microscopic and macroscopic is therefore based on the level of detail. Macroscopic models often use an equilibrium relationship between speed and flow. This equilibrium relationship is commonly known as the fundamental diagram (Greenshield 1935).

The earliest macroscopic model is the LWR model, which is a first-order kinematic wave model that was simultaneously introduced by Lighthill and Whitham (1955) and Richards (1956). It describes the flow based on the assumption that traffic is a continuum and obeys the physical law for mass conservation. Using the density k, flow q and average speed u at position x and time t, the continuity equation is given by:

$$\frac{\partial k(x,t)}{\partial t} + \frac{\partial q(x,t)}{\partial x} = 0, \tag{1}$$

with

$$q(x,t) = u(x,t)k(x,t) \tag{2}$$

and

$$u(x,t) = U(k(x,t)) \tag{3}$$

stating that velocity u is given by the fundamental diagram U.

The solution to the mentioned system of equations has two important properties: hyperbolicity and anisotropy. Hyperbolicity indicates that perturbations in the flow travel as waves through time and space, so they are not instantaneously felt in the whole domain. Anisotropy means that traffic flow is influenced by the traffic state in front and not from the back. For this, the wave speed of perturbations should never exceed the maximum velocity. Anisotropy requires the model to be weakly hyperbolic, which is the case if when the velocity function is nonincreasing (Zhang et al. 2006; van Wageningen-Kessels et al. 2013). In the simulation, the solution of the kinematic wave model is approximated using a numerical scheme. The LWR model is commonly solved using Godunov's method, which is a finite difference scheme (Godunov 1959), but also other methods have been applied.

The LWR model is both loved and criticised for its simplicity. The main imperfection is that the model describes equilibrium states only, which implies that changes in traffic state result in instantaneous speed adjustments. In reality, traffic is often in non-equilibrium and a reaction time is observed for acceleration and deceleration. This deficiency has been partially addressed in higher-order models by replacing the fundamental diagram with a velocity function that includes acceleration behaviour based on driver anticipation, relaxation and traffic inertia, e.g. Payne (1971). After critique that the higher-order model is not anisotropic and therefore unrealistic at traffic discontinuities (Daganzo 1995), several adjustments are proposed to incorporate changes in e.g. density (Aw and Rascle 2000), headway (Berg, Mason, and Woods 2000), velocity distribution (Zhang 2002), speed gradient (Gupta and Katiyar 2006) and driver physiological response (Khan et al. 2019). Despite these developments in second-order models, the first-order kinematic wave model remains an effective and popular method to describe traffic flow as long as traffic flow phenomena, e.g. capacity drop and stop-and-go waves, are not required.

The aforementioned models describe homogeneous traffic flow. The description of heterogeneous traffic has been addressed in the development of multi-class models by distinguishing traffic type using e.g. different velocities (Wong and Wong 2002; Zhang et al. 2006), vehicle size (Chanut and Buisson 2003; Logghe and Immers 2008), and impact based on velocity using static (Ngoduy and Liu 2007) and dynamic passenger car equivalent (pce) values (van Lint, Hoogendoorn, and Schreuder 2008). Furthermore, developments have been made in describing traffic situations with multiple lanes, e.g. the '2-pipe regime' with slugs and rabbits (Daganzo 2002), modified speed–density relation based on lane-changing (Jin 2010) and utility-driven lane changes (Shiomi et al. 2015). The disordered traffic situation, in which lane discipline is lacking, has been captured in continuum models using e.g. available space (Benzoni-Gavage and Colombo 2003; Nair, Mahmassani, and Miller-Hooks 2011; Fan and Work 2015) and lateral distances (Gupta and Dhiman 2014).

Heterogeneous models capture the characteristics of different traffic types and the effect of their interaction on the overall flow. Slow vehicles, such as buses (Lebacque, Lesort, and Giorgi 1998) and lorries (Muñoz and Daganzo 2002), are considered as moving bottlenecks for cars, whereas the impact of pedestrians on car traffic is addressed in Daganzo and Knoop (2016). The model of Fan and Work (2015) includes the characteristic trait of small vehicles, i.e. motor cyclists, to manoeuvre through congestion, maintaining a higher speed than cars. This interaction between cars and powered two-wheelers is further developed by Gashaw, Goatin, and Harri (2018), whose model also takes into account that a higher share of two-wheelers results in a lower speed at similar road occupancy. To our knowledge, bicyclists have not been included yet in macroscopic models. However, there are examples

of microscopic models that include bicycles, e.g. the individual-following model by Tang, Huang, and Shang (2010) and the cellular automata model by Luo et al. (2015).

All macroscopic flow models describe traffic using the relation between position, time and vehicle number. Three different representations of traffic arise by fixing one of the three variables (Laval and Leclercq 2013). The most common one is the Eulerian coordinate system, which fixes the vehicle number and visualises the number of vehicles that have passed a location at a certain time. Another well-known representation is the Lagrangian coordinate system in which time is fixed. Here, the time at which vehicles pass a certain location is simulated, resulting in trajectories. The third and least common representation fixes the position and describes the time at which vehicles cross a certain location.

Although the Eulerian method is most commonly used, the Lagrangian method has been successfully applied to numerically solve the kinematic wave model as well. This has been done for homogeneous traffic (Leclercq 2007; Wu et al. 2014), as well as mixed traffic including trucks (van Wageningen-Kessels et al. 2011) and motor cyclists (Gashaw, Harri, and Goatin 2018). Examples of the Lagrangian method applied to second-order flow models are Greenberg (2001, 2004); Zhang, Wu, and Wong (2012). In the macroscopic approach, the Lagrangian method calculates the traffic evolution for platoons consisting of multiple vehicles, whereas the microscopic approach gives the trajectories of individual traffic participants. The macroscopic model reduces to a microscopic car-following model when the platoon size is reduced to one vehicle only, as shown e.g. by (Aw et al. 2002) and Leclercq (2007). Information travels downstream only in the Lagrangian Godunov scheme, making it less prone for errors due to numerical diffusion. Using the Lagrangian methods therefore results in a more robust model compared to the Eulerian scheme where information travels both up and downstream.

Based on the above, we have identified the gap in literature that bicycles are not yet represented in macroscopic traffic flow models, while they are an important part of daily traffic in countries such as The Netherlands and China. The common feature in the above-mentioned models is that a fastest class is assumed; one class, i.e. the passenger car, is assigned to have the highest speed irrespective of prevalent traffic conditions. This assumption is limiting when representing bicyclists, since they are able to switch into being the faster class when manoeuvring forward in congestion. This occurs, for instance, in the situation where the road is wide enough for a car and cyclist to move alongside each other, and the cyclists can pass a queue of stopped cars. We include this phenomenon by introducing class-specific speed functions in the first-order macroscopic model, which depends on the density of all modes. We use the Lagrangian method because of its modelling accuracy.

3. Lagrangian model

The starting point of our model is the continuity equation in Eulerian coordinates, Equation (1), which states that changes in density over time should match the change in flow over space, indicating that vehicles should not suddenly appear or disappear from the road. To rewrite into Lagrangian coordinates, we use the spacing s instead of the density k as the main variable. Spacing is equivalent to space headway and is defined as the average distance between travellers belonging to the same entity. Furthermore, the spacing is

inversely proportional to the density,

$$s = \frac{1}{k}. \tag{4}$$

The spacing can also be expressed as the partial derivative of the position x to vehicle number n:

$$s = -\frac{\partial x}{\partial n}. \tag{5}$$

Here, the negative sign results from the choice in the numbering of traffic units. These numbers are assigned when traffic units pass a certain position. When selecting a position further along the road (larger x), less vehicles will have passed it (lower n), resulting in a negative sign for the change in n.

When substituting Equation (4) into the Eulerian continuity equation, we get:

$$\frac{\partial}{\partial t}(1/s) + \frac{\partial}{\partial x}(v/s) = 0 \tag{6}$$

Now, using the quotient rule, Equation (5) and the Lagrangian time derivative

$$\frac{\mathrm{D}}{\mathrm{D}t} = \frac{\partial}{\partial t} + v\frac{\partial}{\partial x}, \tag{7}$$

we retrieve the continuity equation expressed in Lagrangian coordinates:

$$\frac{\partial s}{\partial t} - s\frac{\partial v}{\partial x} + v\frac{\partial s}{\partial x} = 0 \quad \Rightarrow \quad \frac{\mathrm{D}s}{\mathrm{D}t} + \frac{\partial v}{\partial n} = 0. \tag{8}$$

The Lagrangian continuity equation states that speed differences between traffic units coincide with changes in their spacing over time. In other words, when two following vehicles initially go at equal speed and the first one slows down, the distance between the two vehicles should decrease.

We now extend the model to describe multiple classes, similar to the multi-class LWR model expressed in Eulerian coordinates Wong and Wong (2002). The conservation equation holds separately for each class u and all variables are class-specific except for time:

$$\frac{\mathrm{D}s_u}{\mathrm{D}t} + \frac{\partial v_u}{\partial n_u} = 0. \tag{9}$$

The density of different classes are not combined into one effective density but treats them independently instead. In practice, this implies that traffic participants of each class can move alongside each other as if they are using separate sections of the road. The interaction between classes is included in the model via the speed function, which will be elaborated in Section 5.

In the numerical implementation, both time and traffic units are discretised in finite steps, while space remains a continuum. Although more classes are possible, we continue with two only, being cars ($u = c$) and bicyclists ($u = b$). The traffic units within these classes are grouped into platoons of a certain size. More details are provided in the following section.

4. Numerical implementation

The Lagrangian continuity Equation (9) is a hyperbolic equation which can be solved numerically using the Godunov scheme. Following the works of Leclercq (2007) and van Wageningen-Kessels et al. (2011), we use an explicit time-stepping scheme to solve the continuity equation, resulting in the following discretised equation:

$$s_{u_i}^{t+1} = s_{u_i}^{t} + \frac{\Delta t}{\Delta n}(v_{u_i-1}^{t} - v_{u_i}^{t}). \tag{10}$$

This equation states that the spacing s in platoon i of class u in the following time step $(t+1)$ can be retrieved by taking the spacing at time t and add it to the difference in speed (v) of subsequent platoons (i and $i-1$), corrected with the time step Δt divided by the number of traffic units in a platoon Δn. To ensure stability and convergence of (10), the CFL condition should be met, which limits the distance a platoon can travel downstream within one timestep (van Wageningen-Kessels 2013). This condition is given by:

$$\frac{\Delta t}{\Delta n}\max|\frac{dv}{ds}| \leq 1. \tag{11}$$

The length of platoon i stretches between positions x_{u_i} and $x_{u_{i+1}}$ and the corresponding spacing within that platoon equals its length divided by its size:

$$s_{u_i} = \frac{x_{u_i} - x_{u_{i+1}}}{\Delta n_u}. \tag{12}$$

Using this discretisation for spacing, we can express the discretised continuity Equation (10) in position x_u which simplifies the simulation, resulting in Eq. (13). The new position x of platoon i and class u is retrieved by adding up the previous position and the distance travelled within the time step Δt.

$$x_{u_i}^{t+1} = x_{u_i}^{t} + v_{u_i}^{t}\Delta t, \tag{13}$$

The change in position is based on the speed v, which in turn depends on the spacing of all classes in the previous time step. In our case, we use two classes, bicycles b and cars c:

$$v_u^{t+1} = V_u(s_b^t, s_c^t), \tag{14}$$

where V_u is the speed function specified by Equation (18) and (19) in Section 5.

The position and speed are given for the first car or cyclist of a platoon, which is defined here as a platoon of dn traffic participants. When the platoon size equals 1, the scheme is basically a microscopic car-following model. This equivalence has been demonstrated by Leclercq (2007) and Zhang, Wu, and Wong (2012). In the macroscopic approach, the platoon size exceeds 1 but it is not restricted to positive integers. Numerically, the platoon size consists of 1.43 or 15.43 traffic participants. However, using decimals would come at the cost of an intuitive physical interpretation of the modelling results. An example of the numbering of platoons, positions and spacings are visualised in Figure 1(a). An additional position is added (x_{u_n}) to mark the end of the last platoon and to ensure that a spacing can be calculated for the area following the last platoon.

A choice is made on how the positions of the N platoons influence the spacing, which influences the speed. Since the speed of a car or cyclist in a platoon is influenced mostly by

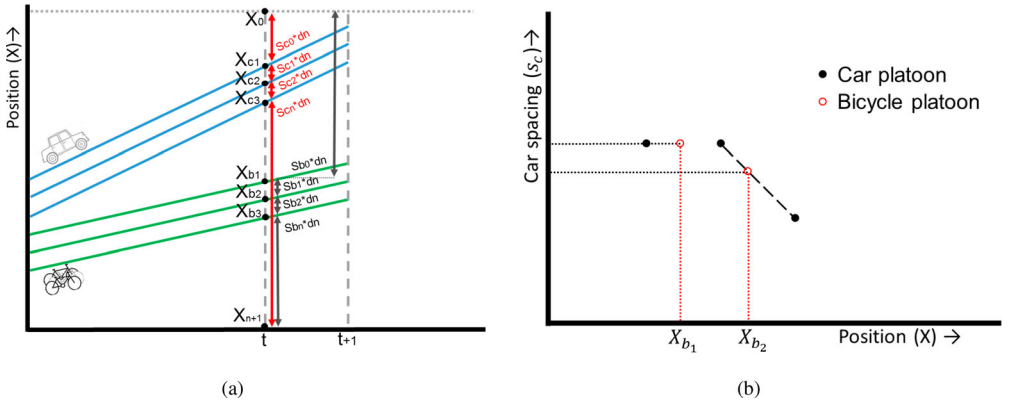

Figure 1. Sketch showing the numbering of the position x and spacing s for two platoons of cars and cyclists (a) and the linear interpolation to retrieve the car spacing at the positions of the bicycle platoons (b).

what happens in front of the platoon, we argue that the downstream spacing is mostly of influence to the speed and to a lesser extent the spacing within the platoon. This way we ensure anisotropy in the numerical scheme. We use the downstream spacing for calculating the speed and the speed Equation (14) is further specified to:

$$v_{u_i}^{t+1} = V_{u_i}(s_{b_{i-1}}^t, s_{c_{i-1}}^t). \tag{15}$$

This equation requires as input the spacing of both classes at the position of a platoon. For one of the classes, the spacing retrieved by Equation (12) can directly be used. However, the spacing of the other class is unspecified yet because the values are known for different x-positions. Therefore, the spacings of the other class need to be determined which is done via linear interpolation. Giving the example of finding the car spacing at the position of a bicycle platoon, the linear interpolation is performed using the car spacing as base for the positions of the car platoons. Figure 1(b) presents a visualisation of this process.

Using the spacing of the downstream area of the platoon comes with a challenge; the spacing in front of the first platoon cannot be determined using Equation (12) without implementing additional boundary conditions. For this purpose, two additional x-positions are predefined which are similar for both classes: x_0 at a position very far away and x_{n+1} at $x = 0$, see Figure 1(a). The first boundary condition ensures that the first platoon always experiences an empty road, while the second condition ensures an empty road after passing of the last platoon.

5. Class-specific speed functions

A main contribution of this work is that the model can handle class-specific speed functions which depend on densities of both classes. In a first-order macroscopic model, the speed function is typically provided by a fundamental diagram, describing the equilibrium relation between the aggregated variables spacing, speed and flow rate. The speed is typically given by the function V that depends on the density and in our case on spacing. In our multi-class situation, the class-dependent fundamental diagram is based on the spacing

Table 1. Characteristic values used in the speed functions: jam spacing s_j, critical spacing s_{cr}, free flow speed v_f and reduced speed v_{red}

	s_j (m)	s_{cr} (m)	v_f (m/s)	v_{red} (m/s)
cyclists	1.5	4.5	5.0	2.0
cars	5.0	10	9.0	-

distribution of both cars and cyclists. Previous work in literature has tackled this multi-dependency by introducing a pce value for each class and calculating the speed based on the number of pce present, $v = V(s_{pce})$.

This study takes an alternative approach using two-dimensional speed functions. The main thought underlying this idea is that at a given generalised density, the speed of cars is fixed, while the speed of cyclists can vary depending on the traffic state, e.g. due to their ability to manoeuvre along a queue of cars. This feature of mixed traffic cannot be captured accurately by a model based on pce value, since this assumes the reference class to always be the fastest moving class. To model the characteristics of both classes correctly, this study introduces class-specific two-dimensional speed functions, which describes the speed of a class, based on the spacing of both cars and cyclists separately, so $v = V(s_c, s_b)$.

The framework presented here can handle various shapes of the fundamental diagram $V(s_c, s_b)$. The starting point for our two-dimensional speed functions is the triangular fundamental diagram in flow-density for single-class traffic flow (Daganzo 1994). In the speed-spacing format, this function is given by:

$$V_u(s_u) = \begin{cases} 0 & \text{if} \quad s_u = s_{u,j} \quad [1] \\ (s_c - s_{c,j})w_u & \text{if} \quad s_{u,j} < s_u \leq s_{u,cr} \quad [2] \\ v_{u,f} & \text{if} \quad s_u > s_{u,cr} \quad [3] \end{cases} \tag{16}$$

with w the wave speed of traffic state characteristics, given by:

$$w_u = \frac{v_{u,f}}{s_{u,cr} - s_{u,j}}. \tag{17}$$

Equation (16) states that the traffic entities of class u are at stand still ($v = 0$) when the jam spacing ($s_{u,jam}$) is reached, their speed gradually increases with spacing until the desired speed ($v_{u,f}$) is reached at the critical spacing ($s_{u,cr}$), and continue to travel at the desired speed for larger spacings. The characteristic values for jam spacing, critical spacing and free flow speed used in this study are presented in Table 1. Figure 2 presents the resulting single-class speed-spacing diagram of cars and bicycles when no other class is present. To connect the two classes, additional cased are added to (16) while trying to maintain a linear expression where possible. This has resulted in the class-specific speed functions for bicycles (18) and cars (19).

For the speed of bicycles, a condition is introduced to reduce the speed to $v_{b,red}$ when cyclists are passing a queue of cars (18.4). Condition (18.5) is included to ensure that the cycling speed does not exceed the reduced speed when cars are slowed down in congestion but not standing still. Equation (18.6) is added to ensure a smooth transition at the boundaries between the reduced speed and the speed reduction caused by decreasing bicycle spacing (18.2). For cars, two additional rules are introduced. First, cars cannot overtake when there are too many cyclists on the road, and they have to adapt their speed to

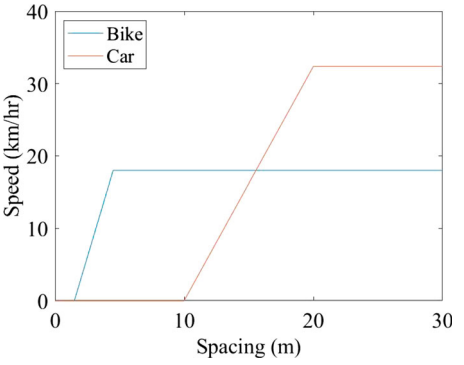

Figure 2. Single-class speed functions for cars and bicyclists.

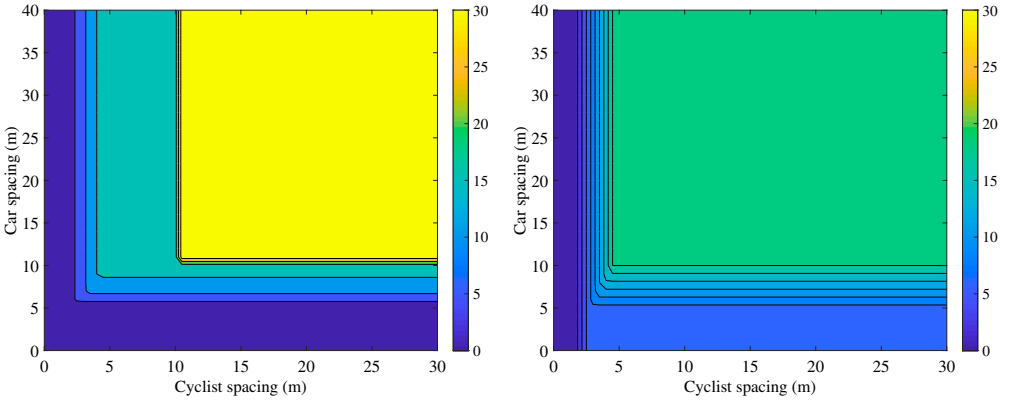

Figure 3. Two-dimensional speed functions for cars (a) and bicyclists (b).

match the cyclist' speed (19.2). Second, when cyclists are sparsely present, i.e. $s_b > a$, sufficient space for cars is available to move in between and overtake at a reduced speed (19.4). We assume this sufficient spacing to be 10 m ($a = 10$ m). The parameter w_{bc} is the tangent of the connecting line between the reduced and free flow speed of bicycles, given by Equation (20). A contour plot of the two-dimensional speed functions are shown in Figure 3.

The class-specific speed functions presented here are non-decreasing with spacing ($\partial v/\partial s \geq 0$), which according to van Wageningen-Kessels (2013) should ensure the model to be weakly hyperbolic and therefore able to show anisotropic behaviour. Further investigation of the hyperbolicity of the model is not performed.

$$V_b(s_b, s_c) = \begin{cases} 0 & \text{if} \quad s_b = s_{b,\mathrm{j}}, \quad s_c > s_{c,\mathrm{j}} & [1] \\ (s_b - s_{b,\mathrm{j}})w_b & \text{if} \quad s_{b,\mathrm{j}} < s_b \leq s_{b,\mathrm{cr}}, \quad s_c > s_{c,\mathrm{j}} & [2] \\ v_{b,\mathrm{f}} & \text{if} \quad s_b > s_{b,\mathrm{cr}}, \quad s_c > s_{c,\mathrm{j}} & [3] \\ v_{b,\mathrm{red}} & \text{if} \quad s_b > s_{b,\mathrm{cr}}, \quad s_c = s_{c,\mathrm{j}} & [4] \\ \min(v_{b,\mathrm{red}}, (s_b - s_{b,\mathrm{j}})w_b) & \text{if} \quad s_{b,\mathrm{j}} < s_b \leq s_{b,\mathrm{cr}}, \quad s_c \leq s_{c,\mathrm{j}} & [5] \\ \min\Big((s_b - s_{b,\mathrm{j}})w_b, \\ \quad v_{b,\mathrm{red}} + w_{bc}(s_c - s_{c,\mathrm{cr}})\Big) & \text{if} \quad s_{b,\mathrm{j}} < s_b \leq s_{b,\mathrm{cr}}, \quad s_{c,\mathrm{j}} < s_c \leq s_{c,\mathrm{cr}} & [6] \end{cases} \tag{18}$$

$$V_c(s_b, s_c) = \begin{cases} 0 & \text{if} \quad s_c = s_{c,\mathrm{j}} \quad s_b > s_{b,\mathrm{j}} \quad [1] \\ \min(V_b, (s_c - s_{c,\mathrm{j}})w_c) & \text{if} \quad s_{c,\mathrm{j}} < s_c \leq s_{c,\mathrm{cr}} \quad s_b > s_{b,\mathrm{j}} \quad [2] \\ v_{c,\mathrm{f}} & \text{if} \quad s_c > s_{c,\mathrm{cr}} \quad s_b > a \quad [3] \\ \min(v_{c,\mathrm{f}}, V_b) & \text{if} \quad s_c > s_{c,\mathrm{cr}} \quad s_b \leq a \quad [4] \end{cases} \tag{19}$$

$$w_{bc} = \frac{v_{b,\mathrm{f}} - v_{b,\mathrm{red}}}{s_{c,\mathrm{cr}} - s_{c,\mathrm{j}}} \tag{20}$$

6. Case study

To illustrate the working of the model, we consider several situations which occur on unidirectional urban streets with mixed bicycle–car traffic. A specific example is a so called 'cycling street' which is gaining popularity in The Netherlands. The traffic behaviour has specific characteristics resulting from the property that bicyclists are prioritised over car drivers. No uniform design of a cycling street exists but it is typically wide enough for cars to overtake cyclists. However, cars are considered as guests on the road and have to slow down when cyclists are present. Furthermore, cars cannot overtake when the cyclist density exceeds a certain threshold and as a result, the cars have to match the cyclists' speed. When cars are moving slowly in a queue there is enough space for cyclists to carefully pass the queue and create their own queue closer to an intersection. The speed limit on this cycling street is 30 km/ h.

In the following three cases, we follow several platoons of five traffic units in space and time ($\Delta n = 5$) and the simulations are performed with time steps of two seconds ($\Delta t = 2$ s). The speed is given by Equations (18) and (19) and the characteristic values in the speed functions are presented in Table 1.

6.1. Little to no interaction

We consider a situation with low demand for the purpose of face validation. All traffic participants can move at their maximum allowed speed and the spacing is large. As a result, the two classes have sufficient space to manoeuvre freely and are unhindered by each others presence. This is the case when we set the initial spacing of both classes to 20 m, which results in a total platoon length of 100 m.

Two cases can occur depending on the starting positions, displayed in Figure 4; either the cars have a head start over the bicycles (a) or the other way around (b). In both cases, there are two platoons of cars and three platoons of cyclists. In the primary case, the cars are given a head start of 350 m. As a result, no interaction between the two classes takes place since the desired speed of cars is higher than that of cyclists causing a rapid divergence of the two classes. Interaction does occur in the second case where the starting positions are switched and the cyclists have a 350 m head start over the cars. Since cars have a higher desired speed, the first platoon of cars catches up with the final platoon of cyclists. Figure 4(b) shows that this happens after approximately 40 s in the simulation. The spacing of the cyclists, however, is sufficiently large and cars can overtake without having to reduce their speed. Note that the speed limit on the bicycle road is 30 km/ h, which is

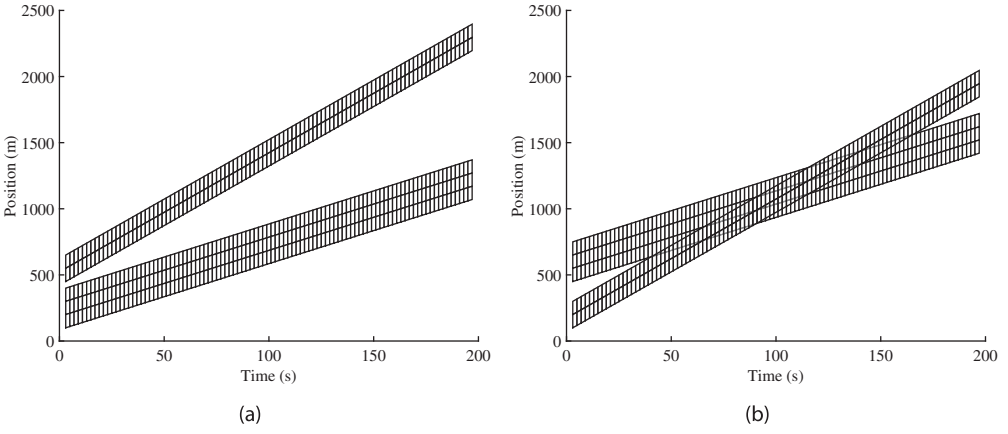

Figure 4. Simulation results for low demand situation ($s_b(t_0) = s_c(t_0) = 20$ m), showing no speed adjustments when cars have a head start over cyclists (a) and cyclists have a head start over cars (b).

considered a safe speed to overtake and no further speed reduction is required. In our simulation it takes about 170 s before all cars have passed the cyclists and the two classes start to diverge.

6.2. Interaction and adjustment by cars

Interaction takes place when more cyclists are occupying the road and their space headway is decreased. For visualisation purposes, we only consider two car and three bicycle platoons but the model will work for any number of platoons. The initial spacing for cars remains 20 m, while the bicycle spacing is decreased, resulting in a more compact platoon length.

Different interactions take place depending on the exact initial spacing. This is best visualised when the initial bicycle spacing is set close to the threshold for interaction, which is $a = 10$ m according to Equation (19). The initial spacing is set to 10.2 m in Figure 5(a) and 10 m in Figure 5(b). As a result, the cars overtake the bicycles with reduced speed in the first case and have to match the cycling speed in the latter case. The speed reduction is visualised by the magenta coloured cells which intensify when the reduction increases. In both cases, the cyclists start with a 350 m head start over the cars, and they can move unhindered and at their desired speed throughout the simulation.

The magenta colouring in Figure 5(a,b) illustrates that the speed adaptation sets in before the complete platoon has reached the cyclists. Also, in Figure 5(a) can be seen that the speed increases already before all cyclists are overtaken. This results from our choice in the numerical implementation to determine the speed based on the spacing in front (Equation (15)), which can be interpreted as anticipation behaviour. As a result, the car spacing after overtaking the cyclists is larger than before the cars reached the cyclists.

6.3. Queuing situations

Both cyclists and cars have to adjust their speed in congested situations where the spacing reduces to values below the critical density. This is included in the simulation by introducing

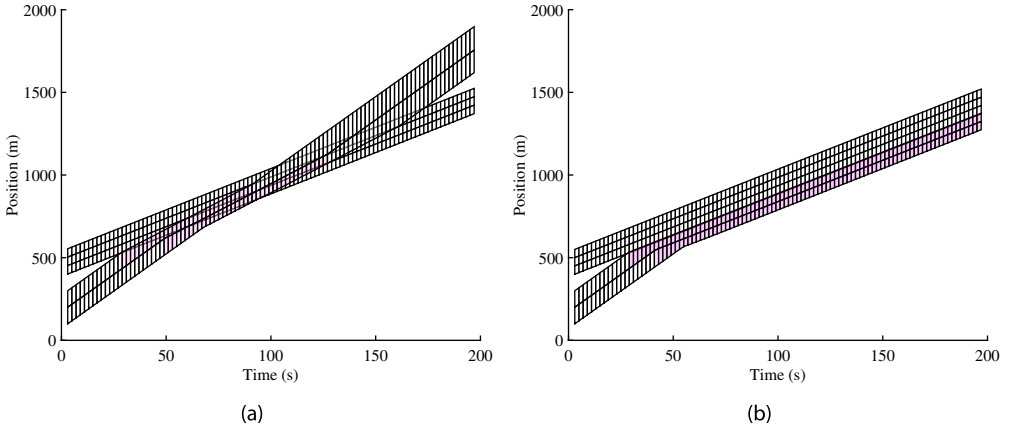

Figure 5. Simulation results for different demand situations. When initial spacings are $s_b(t_0) = 10.2$ m and $s_c(t_0) = 20$ m, cars can still overtake cyclists but at a reduced speed (a) and when initial spacings are $s_b(t_0) = 10$ m and $s_c(t_0) = 20$ m cars have to match the speed of cyclists (b). The magenta colouring appears when the speed is reduced and is more intense for lower speeds.

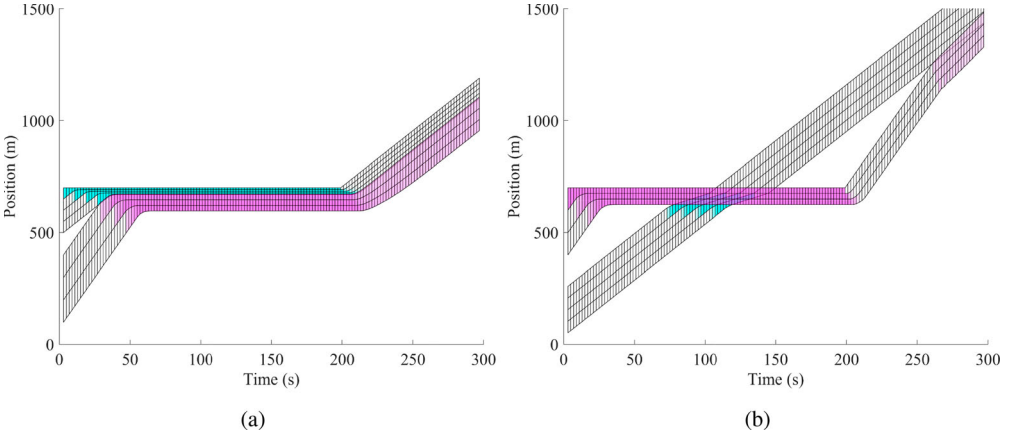

Figure 6. Simulation results for queuing situations. In (a) $s_b(t_0) = 10.2$ m and $s_c(t_0) = 20$ m and the cyclist have a head start of 450 m. In (b) $s_b(t_0) = 10.4$ m and $s_c(t_0) = 20$ m and the cars have a head start of 300 m. The cyan and magenta colouring appear when the speed is reduced for, respectively, cyclists and cars.

a temporary obstruction; the first platoon is enforced to stop in the first time step causing queue formation behind it. Again, two cases can occur based on the starting positions of the two classes. When the cyclists have a head start over the cars, the first platoon of cyclists is stopped creating a growing queue of first cyclists and then cars, see Figure 6(a). The speed reduction of the cars and cyclists is visualised by the colours magenta en cyan, respectively; no colour is shown when speed coincides with the desired speed. In total, three car and four platoons are followed in time and space. The first cyclists have a 450 m head start over the first cars. After some time in the simulation, the first cars catch up with the last cyclists and the cars have to reduce speed until they come to a complete stop. The bottleneck is removed after 200 s after which the cyclists restart moving and the queue is gradually

cleared. The cyclists quickly move at their desired speed again, but the spacing is too small for the cars to overtake.

A different situation occurs when the starting positions are switched around and the first car platoon is stopped instead. The cyclists can pass the queue of cars but have to do so at a reduced speed. The cars have a head start of 300 m over the cyclists and it takes some time for the first cyclists to catch up with the last cars. When looking closely at the colouring, the cyclists are reducing speed well before they reach the actual position of the queue, and they are increasing in speed before the queue is actually passed. This results from the assumption that the speed is influenced most by the spacing in front of the traffic participants instead of the spacing at their current position. When the cars start moving again after the obstruction is removed, the cars can first move at their maximum allowed speed until they catch up with the cyclists and reduce their speed to gradually overtake them.

6.4. Discussion

The face validation of the three cases show that the model can accurately handle various conditions that occur in mixed traffic situations where bicycles and cars share the same infrastructure. The main feature is that both classes can be the fastest moving one, depending on the traffic state. Furthermore, the model includes anisotropy by considering only the spacing of all classes in front of the current position to adjust the speed. This modelling approach leads to plausible results including anticipation; traffic participants slow down before reaching a queue and accelerate when a queue is about to dissolve.

When comparing our modelling outcome to available research on mixed bicycle–car traffic, we have two observations. Our model includes a two-way interaction between cars and cyclists; the speed of cars is influenced by the presence of bicycles and vice versa. This property is an improvement compared to the individual-following model by Tang, Huang, and Shang (2010), which includes one-way interaction only. However, the bicycle–car interaction in our model is based on space headway only and does not take the lateral spacing into account, which is the case in the cellular automata model by Luo et al. (2015). To include the interaction due to lateral distance, the future development of our model could include a fundamental diagram based on an area density.

The presented model is tested solely to qualitative criteria and has not yet been validated with observational data. The model is tested for the Dutch cycling street scene but could also be applied in other mixed traffic situation, e.g. where lane discipline is lacking. However, this would require an adjustment to the speed functions. The development of a more general description of the speed function will be beneficial for the applicability of the presented macroscopic flow model.

7. Conclusion

A first-order multi-class macroscopic flow model is presented to describe mixed bicycle–car traffic. The model uses class-specific speed functions, enabling each class to be the fastest moving one depending on density. This trait facilitates the modelling of e.g. congested situations where cyclists can manoeuvre along a queue of cars. The presented model is specifically relevant for shared street situations, which typically occur in urban

environments. Three test cases show the ability of the model to handle various traffic flow conditions that occur in mixed traffic situations where bicycles and cars share the infrastructure. The model shows anisotropic behaviour by considering the spacing of all classes in front to adjust the speed. This modelling approach leads to plausible results including anticipation; traffic participants slow down before reaching a queue and start accelerating when a queue is about to dissolve.

The working of the model has been successfully tested based on qualitative criteria, showing the expected behaviour of mixed bicycle–car traffic. The next step would be to perform a validation of the model to quantitatively test it against observational data. These data, however, are not yet available. Furthermore, the mathematical properties of the model could be further investigated, e.g. hyperbolicity. In this study, mixed traffic consisting of bicycles and cars are considered but the model is equally applicable to other configurations of mixed traffic. However, this would require adjustments to the speed functions. Possible applications of the model are estimation of e.g. class-specific travel time and road capacity in a mixed traffic situations, which is all relevant input data to network-wide traffic models and route choice models.

Disclosure statement

No potential conflict of interest was reported by the author(s).

Funding

This research was supported by the ALLEGRO project, which is financed by the European Research Council (Grant Agreement No. 669792) and the Amsterdam Institute for Advanced Metropolitan Solutions.

ORCID

M. J. Wierbos http://orcid.org/0000-0001-8857-4006
V. L. Knoop http://orcid.org/0000-0001-7423-3841
S. P. Hoogendoorn http://orcid.org/0000-0002-1579-1939

References

Aw, A., A. Klar, M. Rascle, and T. Materne. 2002. "Derivation of Continuum Traffic Flow Models From Microscopic Follow-the-Leader Models." *SIAM Journal on Applied Mathematics* 63 (1): 259–278.

Aw, A., and M. Rascle. 2000. "Resurrection of 'Second Order' Models of Traffic Flow." *SIAM Journal on Applied Mathematics* 60 (3): 916–938.

Benzoni-Gavage, S., and R. M. Colombo. 2003. "An N-populations Model for Traffic Tlow." *European Journal of Applied Mathematics* 14 (5): 587–612.

Berg, P., A. Mason, and A. Woods. 2000. "Continuum Approach to Car-Following Models." *Physical Review E – Statistical Physics, Plasmas, Fluids, and Related Interdisciplinary Topics* 61 (2): 1056–1066.

Chanut, S., and C. Buisson. 2003. "Macroscopic Model and Its Numerical Solution for Two-Flow Mixed Traffic with Different Speeds and Lengths." *Transportation Research Record: Journal of the Transportation Research Board* 1852: 209–219.

Daganzo, C. F. 1994. "The Cell Transmission Model: A Dynamic Representation of Highway Traffic Consistent with the Hydrodynamic Theory." *Transportation Research Part B* 28 (4): 269–287.

Daganzo, C. F. 1995. "Requiem for Second-order Fluid Approximations of Traffic Flow." *Transportation Research Part B* 29 (4): 277–286.

Daganzo, C. F. 2002. "A Behavioral Theory of Multi-Lane Traffic Flow. Part I: Long Homogeneous Freeway Sections." *Transportation Research Part B: Methodological* 36: 131–158.
Daganzo, C. F., and V. L. Knoop. 2016. "Traffic Flow on Pedestrianized Streets." *Transportation Research Part B: Methodological* 86: 211–222.
Fan, S., and D. B. Work. 2015. "A Heterogeneous Multiclass Traffic Flow Model With Creeping." *SIAM Journal on Applied Mathematics* 75 (2): 813–835.
Gashaw, S., P. Goatin, and J. Härri. 2018. "Modeling and Analysis of Mixed Flow of Cars and Powered Two Wheelers." *Transportation Research Part C: Emerging Technologies* 89: 148–167.
Gashaw, S., J. Harri, and P. Goatin. 2018. "Lagrangian Formulation for Mixed Traffic Flow Including Two-Wheelers." 21st IEEE Conference on Intelligent Transportation Systems, 1956–1961. Maui: IEEE.
Godunov, S. 1959. "Finite Difference Method for Numerical Computation of Discontinuous Solutions of the Equations of Fluid Dynamics." *Matematicheskii Sbornik* 47(89) (3): 271–306.
Greenberg, J. M. 2001. "Extensions and Amplifications of a Traffic Model of Aw and Rascle." *SIAM Journal on Applied Mathematics* 62 (3): 729–745.
Greenberg, J. M. 2004. "Congestion Redux." *SIAM Journal on Applied Mathematics* 64 (4): 1175–1185.
Greenshield, B. 1935. "A Study of Traffic Capacity." In *Highway Research Board Proceedings*, 14 vols, 448–477. Washington, DC: National Research Council.
Gupta, A. K., and I. Dhiman. 2014. "Analyses of a Continuum Traffic Flow Model for a Nonlane-based System." *International Journal of Modern Physics C* 25 (10). Article 1450045.
Gupta, A. K., and V. K. Katiyar. 2006. "A New Anisotropic Continuum Model for Traffic Flow." *Physica A: Statistical Mechanics and Its Applications* 368: 551–559.
Jin, W. L. 2010. "A Kinematic Wave Theory of Lane-changing Traffic Flow." *Transportation Research Part B: Methodological* 44 (8–9): 1001–1021.
Khan, Z. H., T. A. Gulliver, H. Nasir, A. Rehman, and K. Shahzada. 2019. "A Macroscopic Traffic Model Based on Driver Physiological Response." *Journal of Engineering Mathematics* 115 (1): 21–41.
Laval, J. A., and L. Leclercq. 2013. "The Hamilton Jacobi Partial Differential Equation and the Three Representations of Traffic Flow." *Transportation Research Part B* 52: 17–30.
Lebacque, J., J. Lesort, and F. Giorgi. 1998. "Introducing Buses Into First-Order Macroscopic Traffic Flow Models." *Transportation Research Record* 1644: 70–79.
Leclercq, L. 2007. "Hybrid Approaches to the Solutions of the 'Lighthill-Whitham-Richards' Model." *Transportation Research Part B: Methodological* 41 (7): 701–709.
Lighthill, M. J., and G. B. Whitham. 1955. "On Kinematic Waves. II. A Theory of Traffic Flow on Long Crowded Roads." Proceedings of the Royal Society A: Mathematical, Physical and Engineering Sciences, 229 vols, 317–345. London: Royal Society.
Logghe, S., and L. Immers. 2008. "Multi-Class Kinematic Wave Theory of Traffic Flow." *Transportation Research Part B: Methodological* 42 (6): 523–541.
Luo, Y., B. Jia, J. Liu, W. H. K. Lam, X. Li, and Z. Gao. 2015. "Modeling the Interactions Between Car and Bicycle in Heterogeneous Traffic." *Journal of Advanced Transportation* 49: 29–47.
Muñoz, J. C., and C. F. Daganzo. 2002. "Moving Bottlenecks: A Theory Grounded on Experimental Observation." In *Transportation and Traffic Theory in the 21 st Century*, 441–461. Adelaide: Emerald Group Publishing Limited.
Nair, R., H. S. Mahmassani, and E. Miller-Hooks. 2011. "A Porous Flow Approach to Modeling Heterogeneous Traffic in Disordered Systems." *Transportation Research Part B: Methodological* 45 (9): 1331–1345.
National Research Council. 1965. *Highway Capacity Manual*. Washington, DC: The Board.
Ngoduy, D., and R. Liu. 2007. "Multiclass First-Order Simulation Model to Explain Non-linear Traffic Phenomena." *Physica A: Statistical Mechanics and Its Applications* 385 (2): 667–682.
Payne, H. J. 1971. *Mathematical Models of Public Systems*, edited by G. A. Bekey, Vol. 1, 51. La Jolla, CA: Simulation Council.
Richards, P. I. 1956. "Shock Waves on the Highway." *Operations Research* 4 (1): 42–51.
Shalini, K., and B. Kumar. 2014. "Estimation of the Passenger Car Equivalent: A Review." *International Journal of Emerging Technology and Advanced Engineering* 4 (6): 97–102.

Shiomi, Y., T. Taniguchi, N. Uno, H. Shimamoto, and T. Nakamura. 2015. "Multilane First-Order Traffic Flow Model with Endogenous Representation of Lane-Flow Equilibrium." *Transportation Research Part C* 59: 198–215.

Tang, T., H. Huang, and H. Shang. 2010. "A Dynamic Model for the Heterogeneous Traffic Flow Consisting of Car, Bicycle and Pedestrian." *International Journal of Modern Physics C* 21 (02): 159–176.

van Lint, J. W. C., S. P. Hoogendoorn, and M. Schreuder. 2008. "Fastlane: A New Multiclass First-Order Traffic Flow Model." *Transportation Research Record: Journal of the Transportation Research Board* 2088: 177–187.

van Wageningen-Kessels, F. L. M. 2013. "Multi-Class Continuum Traffic Flow Models: Analysis and Simulation Methods." Ph. D. thesis, Delft University of Technology.

van Wageningen-Kessels, F. L. M., H. van Lint, S. P. Hoogendoorn, and K. Vuik. 2011. "Lagrangian Formulation of Multiclass Kinematic Wave Model." *Transportation Research Record: Journal of the Transportation Research Board* 2188: 29–36.

van Wageningen-Kessels, F. L. M., B. vant Hof, S. P. Hoogendoorn, H. van Lint, and K. Vuik. 2013. "Anisotropy in Generic Multi-Class Traffic Flow Models." *Transportmetrica A: Transport Science* 9 (5): 451–472.

Wong, G. C. K., and S. C. Wong. 2002. "A Multi-Class Traffic Flow Model An Extension of LWR Model with Heterogeneous Drivers." *Transportation Research Part A: Policy and Practice* 36 (9): 827–841.

Wu, C. X., P. Zhang, S. C. Wong, and K. Choi. 2014. "Steady-State Traffic Flow on a Ring Road with Up- and Down-Slopes." *Physica A: Statistical Mechanics and Its Applications* 403: 85–93.

Zhang, H. M. 2002. "A Non-Equilibrium Traffic Model Devoid of Gas-like Behavior." *Transportation Research Part B: Methodological* 36: 275–290.

Zhang, P., R. X. Liu, S. C. Wong, and S. Q. Dai. 2006. "Hyperbolicity and Kinematic Waves of a Class of Multi-Population Partial Differential Equations." *European Journal of Applied Mathematics* 17 (2): 171–200.

Zhang, P., C. X. Wu, and S. C. Wong. 2012. "A Semi-Discrete Model and Its Approach to a Solution for a Wide Moving Jam in Traffic Flow." *Physica A: Statistical Mechanics and Its Applications* 391 (3): 456–463.